Construction and Building Materials 213 (2019) 348–359

Contents lists available at ScienceDirect

Construction and Building Materials

journal homepage: www.elsevier.com/locate/conbuildmat

Effect of steel fibers on the performance of concrete made with recycled concrete aggregates and dune sand

Nancy Kachouh, Hilal El-Hassan *, Tamer El-Maaddawy

Department of Civil and Environmental Engineering, UAE University, P.O. Box 15551, Al Ain, United Arab Emirates

HIGHLIGHTS

- Fresh and hardened properties of RCA-based mixes were evaluated.
- Steel fibers effectively enhanced the hardened properties of RCA-based concrete.
- Analytical regression models relating various hardened concrete properties were proposed.

ARTICLE INFO

Article history:
Received 11 November 2018
Received in revised form 26 March 2019
Accepted 8 April 2019

Keywords:
Steel fibers
Dune sand
Recycled concrete aggregate
Fresh properties
Hardened properties
Analytical regression model

ABSTRACT

This paper aims to develop and evaluate the performance of steel fiber-reinforced concrete made with recycled concrete aggregates (RCA) and desert dune sand. Different fresh and hardened properties of RCA concrete mixtures with and without steel fibers were evaluated and compared with those of a mixture made with natural coarse aggregates (NA). Test parameters included the RCA replacement percentage and steel fibers (SF) volume fraction (v_f). Test results showed that the substitution of 30% of NA with RCA in plain concrete mixes did not reduce the design cylinder compressive strength (f'_c), whereas the use of higher percentages of RCA replacement compromised the fresh and hardened properties of the concrete. The addition of SF significantly reduced the adverse effects caused by the inclusions of RCA in the mixes. RCA-based concrete mixtures having 70 and 100% RCA replacements could be produced with f'_c values comparable to that of a NA-based concrete, when minimum v_f values of 1, and 2% were added, respectively. The RCA replacement increased the water absorption and sorptivity but decreased the ultrasonic pulse velocity, bulk resistivity, and abrasion resistance. The addition of SF improved the hardened properties of RCA-based concrete mixes to an extent of exceeding some of those of the NA-based counterpart, as in the case of abrasion resistance. Analytical regression models were introduced to correlate different concrete properties to the 28-day cylinder compressive strength.

1. Introduction

Concrete is one of the most consumed construction materials. It uses significant amount of non-renewable natural resources in the production of its components, aggregates and cement. To sustain the continuous population growth and construction development, more concrete will be required. Consequently, the increasing demand for aggregates raises concerns of the depletion of their current sources and the availability of new sources. At the end of its service life, a concrete structure is demolished, creating massive amounts of construction and demolition waste (CDW) [1]. The concrete waste is mostly disposed of in landfills, instigating serious environmental hazards. The limited space for landfills to contain CDW and the scarcity of natural resources for natural aggregates (NA) promote the concept of reusing this waste by manufacturing RCA as a potential substitute to NA. This promising approach is considered an innovative means to promote the use of sustainable materials in construction.

The usage of concrete made with RCA has been limited to non-structural applications such as roadway subbase [2,3]. This is because RCA has lower strength and elastic modulus and higher water absorption and porosity compared to NA [4,5]. As a result, the incorporation of RCA in concrete mixtures causes a decrease in its mechanical performance compared to its conventional counterpart [6–8]. Çakır [9] studied the effect of using a 100% RCA replacement on the concrete compressive strength. It was concluded that the compressive strength of concrete with a 100% replacement of RCA decreased by approximately 24% compared to that of concrete made of NA. Corinaldesi [10] investigated the

* Corresponding author.
E-mail address: helhassan@uaeu.ac.ae (H. El-Hassan).

https://doi.org/10.1016/j.conbuildmat.2019.04.087
0950-0618/

mechanical properties of concrete made of RCA. The target compressive strength was attainable with up to a 30% replacement of RCA. However, with this RCA replacement, the elastic modulus decreased by 15% compared to that of NA-based concrete. Malešev et al. [11] studied the properties of fresh and hardened concrete made with different replacement percentages of RCA (0%, 50, and 100%). The researchers concluded that the bulk density of fresh concrete, wear resistance, and modulus of elasticity decreased while increasing the quantity of RCA. Furthermore, when the RCA was obtained by crushing a high-strength concrete, the compressive strength was not reduced compared to that of normal-strength concrete. Yet, the properties of concrete made of RCA were affected by the source of RCA used [11,12]. Concrete made of RCA obtained from an unknown source had lower compressive and tensile strengths than those of concrete made of RCA obtained by crushing of concrete structures with known compressive strengths of 30 MPa and 50 MPa [12]. The compressive stress-strain behavior of steel fiber-reinforced concrete and of recycled aggregate concrete had been separately studied previously [13,14].

To counteract the strength reduction when RCA is used in concrete, different measures were proposed such as increasing the cement content, reducing water-to-cementitious material (w/cm) ratio, adding fly ash, removing the old adhered mortar by using a mechanical grinder or by presoaking in water or in acid, strengthening the old adhered mortar attached to the RCA by using pozzolanic solutions or calcium carbonate deposition that can fill the micro cracks inside the adhered mortar, and adding steel fibers (SF) [1,15–17]. Tam et al. [18] proposed a new two-stage mixing approach, whereby part of the mixing water was added to the fine and coarse aggregates before the remaining water was added alongside the cement. Experimental results showed that the compressive and tensile strengths of RCA concrete prepared using this alternative approach were 22% higher than those of conventionally mixed RCA concrete mixtures. Furthermore, previous research has investigated the effect of adding up to 2% SF, by volume, on the properties of RCA concrete mixtures. Results of fiber-reinforced RCA concrete showed that the elastic modulus, tensile strength, toughness and impact resistance increased, while the compressive strength was not significantly affected by the inclusion of fibers, compared with those of NA-based concrete. This was mainly attributed to the random fiber orientation in the concrete mixtures [13,19,20]. The inclusion of SF improved the quality of concrete made of RCA by reducing the development of micro-cracks [21–23]. Carneiro et al. [24] studied the effect of adding 0.75% SF to concrete mixes made with 25% RCA replacement. Experimental results reported an increase in the compressive strength and a more ductile failure, whereby the toughness, measured by the slope of the descending branch of the compressive stress-strain curves, increased. While SF incorporation into RCA concretes seems promising, limited information is available in the literature on the viability of using a SF volume fraction $\geq$2% to improve properties of concrete made with up to 100% RCA replacement percentage. In addition, the majority of previous work altered mixture proportions to attain a target design compressive strength and slump [21,22]. The abrasion resistance of the RCA-based mixtures and the use of the ultrasonic pulse velocity (UPV) and resistivity tests as non-destructive techniques (NDTs) to evaluate the quality of RCA-based concrete has received little attention.

This paper aims to develop and evaluate the performance of concrete made with RCA, desert dune sand and SF as a sustainable construction material for structural application. In this study, RCA were obtained from crushed concrete structures with an unknown strength and were not subjected to any treatment. This scheme provides a more industrially-favored approach that promotes the use of RCA in its as-received conditions. Previous work has generally used natural fine aggregates with coarse RCA; in this research, locally-abundant desert dune sand was employed as fine aggregates to emphasize the contribution towards sustainable construction. Conventional concrete mixture components were proportioned for a 28-day cylinder compressive strength of 30 MPa. The mix proportions were kept constant in all mixtures. NA was replaced by RCA in the order of 30, 70, and 100%, by mass. SF were added in the order of 1, 2, and 3%, by volume, to RCA-based concrete mixes in an effort to improve various hardened properties, including compressive strength, stress-strain response, and modulus of elasticity. The effect of RCA replacement and SF addition on slump, fresh density, and hardened density was also assessed. Further, the water absorption, sorptivity, UPV, bulk resistivity, and abrasion resistance of the mixtures were evaluated. This investigation provides the engineering community a cutting-edge material characterization of steel fiber-reinforced RCA concrete and would serve as a solid platform to build a design methodology for using such a new concrete as a sustainable material for structural applications.

2. Materials and methods

A total of 13 mixes were designed and prepared using different proportions of NA, RCA and SF. The experimental investigation was carried out on 100 mm cubes, 100 $\times$ 200 mm cylinders (diameter and height) and 100 $\times$ 50 mm discs (diameter and thickness) to evaluate different fresh and hardened properties of the concrete mixes. It is worth noting that the ability of concrete to resist abrasion (i.e. Los Angeles abrasion) and penetration of aggressive ions (i.e. absorption, sorptivity, and bulk resistivity), provides an indication on its probable future durability in line with Mehta [25] and ACI Committee 201.2 [26]. The properties of different materials used, concrete mixture proportioning, sample preparation procedures, and performance evaluation tests are presented in the sections below.

2.1. Materials

ASTM Type I ordinary Portland cement (OPC) was used as a binder in the concrete mixtures. Locally-abundant desert dune sand was employed as a sustainable fine aggregate in all mixes. The gradation curves of cement and dune sand are shown in Fig. 1. The coarse aggregates included NA and RCA. While the NA was obtained as crushed limestone with a nominal maximum particle size (NMS) of 19 mm, the RCA were collected from a local concrete recycling plant that crushes construction and demolition waste from old concrete structures with an unknown compressive strength with a NMS of 25 mm. It is worth noting that the plant did not perform any chemical treatment to the obtained RCA nor separated unwanted materials such as façade stones, bricks, ceramics and other debris. The particle size distribution of different mixes/blends of NA and RCA used in this study are shown in Fig. 2. All grading curves were within the upper and lower limit bounds specified by ASTM C33 [27]. Table 1 summarizes the physical properties of fine and coarse aggregates. It is clear that RCA is lighter than NA with a lower specific gravity and dry-rodded density. The former is also more susceptible to abrasion and mass loss due to exposure to magnesium sulfate (soundness). Nevertheless, all measured properties were within the typical limits given by the ASTM standards and/or international design codes [28–31], except the water absorption of the RCA, which was found to be higher. The absorption, measured as per ASTM C127 [32], of RCA was nearly 30 times more than that of NA. To account for such absorption, additional

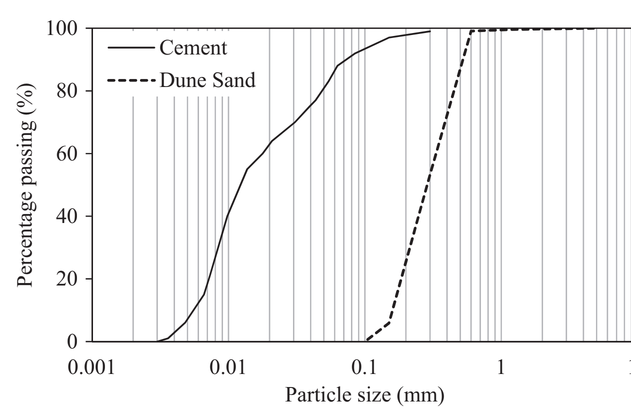

Fig. 1. Particle size distribution of cement and dune sand.

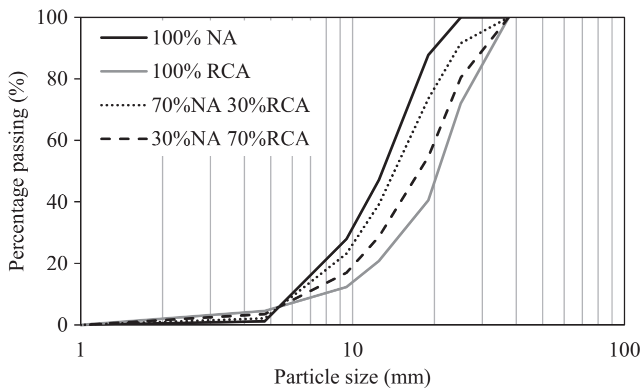

Fig. 2. Particle size distribution of different mixes of NA and RCA.

Table 1
Physical properties of fine and coarse aggregates.

Property	Unit	Standard Test	NA	RCA	Dune Sand
Dry-rodded density	kg/m^3	ASTM C29	1635	1563	1663
Absorption	%	ASTM C127	0.22	6.63	-
Los Angeles abrasion	%	ASTM C131	16.0	32.6	-
Surface area	cm^2/g	ASTM C136	2.49	2.50	116.8
Soundness ($MgSO_4$)	%	ASTM C88	1.20	2.78	-
Specific gravity	–	ASTM C127	2.82	2.63	2.77
Fineness modulus	–	ASTM C136	6.82	7.44	1.45

water was added to the RCA to attain a saturated surface dry (SSD) condition prior to batching into the concrete mix. The double hooked-end SF added in some mixes had a tensile strength of 1345 N/mm^2, Young's modulus of 210000 N/mm^2, mean diameter (d_f) of 0.55 mm, mean length (l_f) of 35 mm, and an aspect ratio (l_f/d_f) of 65 [33].

2.2. Mixture proportioning

The proportions of all concrete mixtures employed in the current study are given in Table 2. The concrete mix design method of ACI 211.1 [34] was first employed to develop a control concrete mixture (i.e. NA-based mixture) with a design cylinder compressive strength (f'_c) of 30 MPa. The cement, dune sand, and water contents were kept constant in all mixtures at 470, 570, and 230 kg, respectively. Due to the slight variation in the specific gravity of the RCA compared to that of the NA, in addition to the inclusion of SF in some mixes, the corresponding volumes of the mixes containing RCA/SF slightly changed. This difference in volume was trivial and negligible, as shown in the last column of Table 2. Samples were labeled as RxSFy, where x denoted the percentage of RCA, relative to total amount of coarse aggregate, and y represented the SF volume fraction. For instance, the control mix without RCA and SF is designated by R0SF0. RCA replacement percentage (RCA, %) was taken as 0%, 30%, 70%, 100%, while SF volume fraction percentage (v_f, %) was altered between 0, 1, 2 and 3%.

2.3. Sample preparation

Concrete sample preparation, including mixing, casting, placing, consolidation, and curing was performed in accordance with the guidelines of ASTM C192 [35]. Specimens were produced using a laboratory mechanical mixer by first mixing in the SF, if any, with the SSD coarse aggregates for 3 minutes. This allowed the SF to uniformly disperse into the mix, especially with high volume fractions of 2 and 3%. Cement and dune sand were later added and further mixed for another 2 minutes. The water was then gradually incorporated into the dry components and mixed together for 2 more minutes to ensure a homogenous and uniform mixture. Fresh concrete samples were cast in two layers and compact-formed using a vibrating table for up to 10 seconds to ensure proper consolidation, as per ASTM C192 [35]. Specimens were then covered with plastic sheets, demolded after 24 hours, and cured in a water tank at 23 ± 2 °C until time of testing. Three replicate specimens were prepared for each test.

2.4. Performance evaluation

Experimental tests were carried out on more than 200 specimens to evaluate the different fresh and hardened properties of the concrete mixes produced in the current study. These tests are described in the following sections.

2.4.1. Slump and density

Fresh concrete slump was measured directly after mixing to evaluate the effect of RCA replacement and SF volume fraction on the workability and rheology of concrete mixes, following the procedure of ASTM C143 [36] and at the recommendation of ACI Committee 544 [37]. Additionally, the fresh (ρ_f) and hardened, 28-day (ρ_h) concrete densities were determined according to ASTM C138 [38] and C642 [39], respectively.

2.4.2. Water absorption

The water absorption test was conducted on 100 × 50 mm concrete disc specimens at the age of 28 days, in accordance with ASTM C642 [39]. Samples were placed in the oven for 24 h until a mass change <0.5% was attained. They were then immersed in water, after which the mass of the saturated surface-dry specimen was determined. The water absorption was calculated using Eq. (1):

$$\text{Water absorption } (\%) = \frac{\text{SSD mass (g)-Oven-dry mass (g)}}{\text{Oven-dry mass (g)}} \text{ x } 100\% \tag{1}$$

2.4.3. Capillary sorptivity

Sorptivity test was performed, as per ASTM C1585 [40], to determine the rate of water absorption. The mass of the 28-day concrete specimen was recorded at different time intervals up to a maximum of 6 hours. Eq. (2) was used to determine the absorption. The slope of the best-fit linear relationship of the absorption plotted against the square root of time from 1 min to 6 h is defined as the initial rate of water absorption, i.e. sorptivity [40].

$$\text{Absorption}, I(\text{mm}) = \frac{\text{Change in mass at time t (g)}}{\text{Exposed area (mm}^2\text{) x Density of water (g/mm}^3\text{)}} \tag{2}$$

2.4.4. Compression behavior

Compressive strength tests were performed on concrete cubes and cylinders in accordance with BS 12390-3 [41] and ASTM C39 [42] procedures, respectively. Axial loads were applied at a loading rate of 7 kN/s using an electro-hydraulic servo controlled machine with a capacity of 2000 kN. Experimental compression stress-strain curves were developed to determine the peak stress, peak strain, and static chord

Table 2
Mix proportions of different concrete mixes.

Mix No.	Mix Designation	Mass (kg)							Volume (m^3)
		Cement	RCA	NA	Dune Sand	Water	SFs	Total	
1	R0SF0	470	0	1130	570	230	0	2400	1.00
2	R30SF0	470	339	791	570	230	0	2400	1.01
3	R70SF0	470	791	339	570	230	0	2400	1.02
4	R100SF0	470	1130	0	570	230	0	2400	1.03
5	R30SF1	470	339	791	570	230	78	2478	1.02
6	R70SF1	470	791	339	570	230	78	2478	1.03
7	R100SF1	470	1130	0	570	230	78	2478	1.04
8	R30SF2	470	339	791	570	230	156	2556	1.03
9	R70SF2	470	791	339	570	230	156	2556	1.04
10	R100SF2	470	1130	0	570	230	156	2556	1.05
11	R30SF3	470	339	791	570	230	234	2634	1.04
12	R70SF3	470	791	339	570	230	234	2634	1.05
13	R100SF3	470	1130	0	570	230	234	2634	1.06

modulus of elasticity, E_c, according to ASTM C469 [43]. The applied axial load was measured employing a 500-kN compression load cell, while the resulting axial strain was recorded using two 60-mm-long strain gauges that were placed vertically at mid-height and on diametrically opposite points of the cylinder's circumference.

2.4.5. Ultrasonic pulse velocity

The UPV test was used as a non-destructive technique to assess the quality of 28-day concrete. Direct UPV tests were conducted on 100 mm cubes samples according to ASTM C597 [44].

2.4.6. Bulk resistivity

Bulk resistivity of concrete is defined as the ability of concrete to resist the diffusion of chloride ions due to electrical current circulation [45]. The rate of penetration of these aggressive ions into the concrete governs its durability [25]. The bulk resistivity depends on the microstructure properties of concrete such as the size and shape of pores [45]. As such, its test results were used to compare probable future durability of concrete mixtures produced in this work. The bulk resistivity test was conducted as per ASTM C1760 [45]. Only plain concrete mixtures without SF were considered in this test. This is because the presence of SF or other embedded electrically conductive materials may yield unrepresentative results. After curing for 28 days, the saturated surface-dry concrete cylindrical specimen was placed in a voltage cell (cells filled with NaCl). Once surface dry state was attained, the cell was loaded with a voltage of 60 ± 0.1 V and the resultant current was measured at 60 ± 5 seconds. Eq. (3) was used to measure the bulk resistivity:

$$\text{Bulk Resistivity } (\text{k}\Omega.\text{cm}) = \frac{\text{Applied voltage (V) x (Avg. sample diameter (mm))}^2}{\text{1273.2 x Current at 1 minute (mA) x Avg. sample length (mm)}} \quad (3)$$

2.4.7. Abrasion resistance

Concrete surfaces are heavily damaged by induced friction and rubbing actions. Abrasion resistance of concrete is defined as the capacity of concrete to resist wearing caused by impact and friction, and could be used to indicate the probable future durability of the concrete produced in this work [25,26]. It depends on the strength of the cementitious paste and aggregate as well as the strength of their interface [46,47]. A Los Angeles abrasion machine was employed to measure the mass loss due to impact and abrasion, as per the procedure prescribed in ASTM C1747 [48]. The mass of each 28-day specimen was recorded before and after the completion of the test. The resistance to abrasion was expressed as the percentage mass loss after 500 revolutions.

3. Experimental results and discussion

3.1. Fresh and hardened density

Fresh and 28-day hardened concrete densities are presented in Table 3. The values ranged from 2248 to 2815 kg/m^3. The density decreased as the RCA replacement percentage increased. Approximately 12 and 14% reduction in fresh and hardened concrete density were respectively observed by increasing the RCA replacement percentage from 0% to 100%, as shown in the fourth and fifth columns of Table 3. It is well known that concrete density is mostly affected by the unit weight of its constituents and air content. Hence, the lower dry-rodded density of the RCA, displayed in Table 1, contributed to the reported reduction in density. The existing mortar attached to RCA could also create a rough, porous surface texture that possibly increased the air content. This decreasing trend was also noticed in concrete mixes with a fixed steel volume fraction, v_f. For example, the addition of 1% SF in R30SF1 increased the fresh density from 2677 kg/m^3 (R0SF0) to 2680 kg/m^3; yet, the replacement of NA by 100% RCA (R100SF1) led to a decrease to 2500 kg/m^3. Additionally, the fresh and hardened concrete densities of mix R30SF3 were 5.2% and 6.2% higher than that of mix R0SF0, respectively, indicating that the effect of RCA replacement on density was less significant in the presence of high amount of SF.

The difference between fresh and hardened concrete densities was calculated and presented in Table 3 (sixth column). An increase in RCA replacement percentage increased the difference between fresh and hardened concrete densities. For mix R100SF0, the difference between fresh and hardened densities was almost double that of the control mix R0SF0, owing to the larger amount of unbound water in RCA concrete. As shown in Fig. 3, a strong correlation (correlation coefficient, R^2 = 0.97) exists between fresh (ρ_f) and hardened (ρ_h) concrete densities. This relationship allows the prediction of the 28-hardened concrete density from the measured fresh concrete density with high accuracy. The relationship between these two properties was established and defined as follows:

$$\rho_h = 0.97\rho_f \quad (4)$$

3.2. Slump

The workability of concrete incorporating different RCA replacement percentages and SF volume fractions was characterized by the slump. As highlighted previously, the cement, dune sand, and water content were kept constant in all mixes. Also, all aggregates were used in SSD condition and did not absorb any of the mixing water. Table 3 presents the slump of fresh concrete with values ranging from 0 to 150 mm. It should be noted that, if natural fine aggregates with density, specific gravity, surface area, and fineness modulus of 1845 kg/m^3, 2.63, 63.5 cm^2/g, and 3.32, respectively, had been used, the slump of the NA-based control mix would have been 175 mm, according to the ACI 211.1 [49]. In comparison, the reported slump of the control mix with dune sand was lower at 150 mm. Apparently, the replacement of natural fine aggregates by dune sand led to a reduction in the slump, possibly due to its larger surface area, higher fine particles contents, and, consequently, higher amount of adsorpted layer water [50].

Table 3
Fresh and hardened density and slump of concrete mixes.

Mix Designation	ρ_f (kg/m^3)	ρ_h (kg/m^3)	Difference in fresh density (%)*	Difference in hardened density (%)*	Difference between fresh and hardened density (%)	Slump (mm)	Change in slump (%)*
R0SF0	2677	2617	–	-	2.2	150	–
R30SF0	2655	2560	−0.8	−2.2	3.6	135	−10
R70SF0	2430	2340	−9.2	−10.6	3.7	117	−22
R100SF0	2357	2248	−11.9	−14.1	4.6	95	−37
R30SF1	2680	2610	0.1	−0.3	2.6	120	−20
R70SF1	2595	2527	−3.1	−3.4	2.6	100	−33
R100SF1	2500	2430	−6.6	−7.2	2.8	86	−43
R30SF2	2750	2690	2.7	2.8	2.2	30	−80
R70SF2	2658	2589	−0.7	−1.1	2.6	25	−83
R100SF2	2600	2530	−2.9	−3.3	2.7	20	−87
R30SF3	2815	2780	5.2	6.2	1.2	0	−100
R70SF3	2710	2675	1.2	2.2	1.3	0	−100
R100SF3	2640	2600	−1.4	−0.7	1.5	0	−100

* with respect to that of R0SF0.

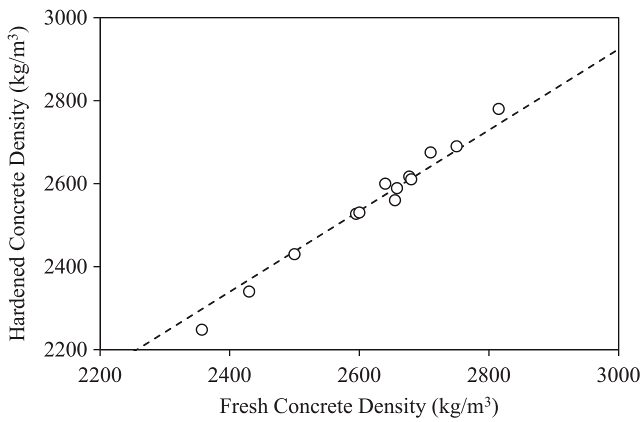

Fig. 3. Relationship between fresh and hardened concrete density.

Results of Table 3 also show that the replacement of NA by RCA reduced the concrete slump. The reduction in slump for the mixes with RCA was calculated with respect to that of the NA-based control mix (R0SF0) and reported in the last column of Table 3. Generally, the slump reduction increased with higher RCA replacement percentage. The replacement of 30% RCA, in the absence of SF, resulted in a 10% slump reduction compared to that of R0SF0. Further increase in the RCA replacement percentage to 100%, in the absence of SF, caused a slump reduction of 37%. Thus, it could be noted that the slump decreased by an average of 3.5% (5.2 mm) for every 10% NA replaced by RCA. Such reduction in slump is owed to the rough surface texture and irregular geometric shape of RCA [6,51,52].

The effect of SF addition on the slump of concrete made with different replacement percentages of RCA was also investigated. Concrete mixes with a 100% RCA replacement and having SF volume fractions of 1, 2, and 3%, exhibited 43, 87, and 100% slump reductions, respectively, compared to that of the NA-based concrete mixture. This corresponded to an average 38.3% loss (57.3 mm) in slump for every steel fiber volume fraction of 1%. With more cement paste needed to cover the SF, less paste was available for workability requirements. It is obvious that the inclusion of 2 and 3% SF, by volume, in the mix had a more severe impact on workability than that caused by the RCA replacement.

3.3. Water absorption and sorptivity

The ability of concrete to absorb water is characterized by its water absorption. Since water is the primary carrier of aggressive ions, concrete resistance to water absorption and transport affects its durability [25]. Accordingly, water absorption and sorptivity (rate of absorption) tests can be used as an indirect evaluation of the concrete porosity and to provide probable future durability of the mixtures produced in this work [53]. Results of water absorption experimental testing are presented in Table 4. The NA-based control specimen (R0SF0) exhibited the lowest water absorption of 5.72%. The substitution of NA by RCA increased the water absorption. RCA replacement of 30, 70, and 100% resulted in 7.83, 8.90, and 9.41% absorption, respectively, representing 37, 55, and 65% respective increases. It can be thus noted that, on average, every 10% RCA replacement caused approximately an 8% increase in the water absorption. This is mainly due to the porous structure of the mortar adhered to the RCA, which provided extensive void sites and caused an increase in water absorption. The addition of SF led to a decrease in the water absorption. Compared to plain concrete counterparts with RCA (R30SF0, R70SF0, and R100SF0), the addition of 1, 2 and 3% SF volume fractions resulted in average reductions in water absorption of 6, 16 and 22%, respectively.

Table 4
Water absorption and initial rate of water absorption.

Mix Designation	RA (%)	SF (%)	Water Absorption (%)	Initial rate of absorption (mm/$\sqrt{s}$)
R0SF0	0	0	5.72	0.023
R30SF0	30	0	7.83	0.030
R70SF0	70	0	8.90	0.037
R100SF0	100	0	9.41	0.040
R30SF1	30	1	7.30	0.029
R70SF1	70	1	8.40	0.034
R100SF1	100	1	8.80	0.038
R30SF2	30	2	6.40	0.025
R70SF2	70	2	7.30	0.029
R100SF2	100	2	8.30	0.033
R30SF3	30	3	5.98	0.022
R70SF3	70	3	6.80	0.026
R100SF3	100	3	7.70	0.030

Based on these results, it can be seen that the inclusion of SF in concrete mixtures densified the concrete matrix and reduced the water absorption of RCA concrete [54].

Sorptivity is the ability of concrete to absorb and transport water through its microstructure by capillary suction. It is mainly affected by the structure and distribution of the pores in the concrete [55]. While the initial sorptivity or rate of absorption represents the sorption process governed by capillary pores, the secondary sorptivity is attributed to that controlled by gel pores [56]. Typically, the initial sorptivity is higher than the secondary sorptivity because water occupies larger capillary pores at a faster rate than smaller gel pores. For this reason, only the initial sorptivity was considered of significant importance in this work. The values of water absorption are plotted against the square root of the time, as shown in Fig. 4. The slope of the sorptivity curve was higher for the first 30 min (42 $s^{0.5}$) than that over the remaining exposure time. This is mainly attributed to the respective filling of large and small pores at early and late stages. Fig. 4(a) illustrates the curves of capillary sorptivity of concrete mixes without SF. An increase in RCA replacement percentage resulted in a higher water absorption and also yielded higher slopes. The effect of SF on the rate of water absorption is shown in Fig. 4(b–d). The slopes and total absorption decreased with a higher addition of SF. While it is well known that fibers in concrete resist water movement [53], it is also believed that they occupy the relatively larger void space in the concrete structure, hence, reducing the rate of water absorption [53,54].

Table 4 presents sorptivity results of concrete specimens at the age of 28 days. For plain concrete mixes (i.e. without SF), it is clear that the sorptivity increased with an increase in the RCA replacement percentage. The addition of steel fibers decreased the sorptivity of the RCA-based mixtures, possibly because they filled the concrete voids [53,54]. In his work, Tamrakar [57] also explained that a high number of steel fibers may enhance the bonding of the concrete matrix, resulting in lower absorption and sorptivity. On average, the addition of SF by 1, 2 and 3%, by volume, resulted in a decrease in the rate of water absorption by 6, 19 and 27%, respectively, compared to that of equivalent RCA-based plain concrete mixes. The obtained reductions in water absorption and sorptivity indicate that the ability of concrete to resist water absorption and transport could be improved by the addition of SF. This is consistent with observations reported in the work of Ramadoss and Nagamani [54].

3.4. Compressive strength

Table 5 presents the compressive strength of concrete mixes at the ages of 3, 7 and 28 days. The effect of subsequent hydration curing on the compressive strength was studied by calculating

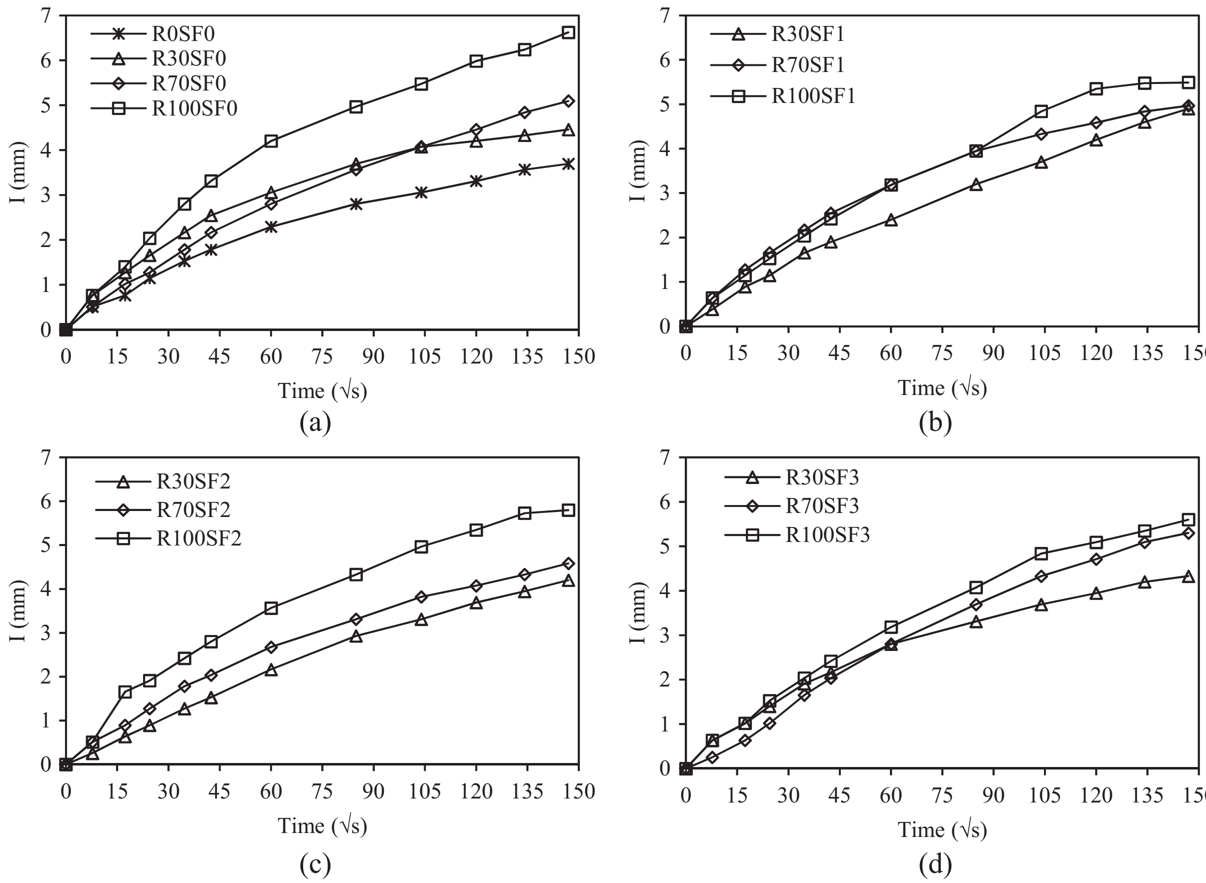

Fig. 4. Capillary sorptivity of concrete mixes over time: (a) SF 0%; (b) SF 1%; (c) SF 2%; (d) SF 3%

Table 5
Compressive strength of concrete cylinders and cubes.

Mix Designation	Compressive Strength (MPa)				Increase in f'_c from 3 to 28 days (%)	Increase in f'_c from 7 to 28 days (%)	f'_c/f_{cu}
	3-Day	7-Day	28-Day	f_{cu}			
R0SF0	23.5	28.4	36.4	42.6	55	28	0.85
R30SF0	17.8	22.1	30.8	33.8	73	39	0.91
R70SF0	13.9	17.1	25.8	27.0	86	51	0.95
R100SF0	13.7	17.2	24.7	26.0	81	44	0.95
R30SF1	15.9	21.7	32.0	35.0	101	48	0.91
R70SF1	13.0	17.3	28.5	30.6	119	64	0.93
R100SF1	12.6	16.8	26.1	28.1	108	55	0.94
R30SF2	20.6	24.2	33.1	36.4	60	37	0.91
R70SF2	17.2	19.5	29.3	31.8	70	50	0.92
R100SF2	16.5	18.4	26.9	28.4	63	46	0.94
R30SF3	22.9	27.5	34.3	38.8	50	25	0.88
R70SF3	20.2	22.9	30.6	33.4	51	33	0.92
R100SF3	19.4	22.6	28.0	29.6	44	24	0.94

the percentage increase in strength from 3 to 28 and 7 to 28 days. Hydration of cement promoted up to 119 and 64% compressive strength gains from 3 to 28 and 7 to 28 days, respectively. Although the initial 3-day strength of the mixes with RCA were lower than that of the NA-based control mix, their strength gain over time was generally higher. It seems that the weak bond between the old and new mortar is mainly responsible for the low early strength. With time, the hydration reaction progressed, providing a better bond and rendering this weakness less prominent. The effect of SF on strength development was also investigated. From Table 5, it can be seen that the inclusion of SF with $v_f \geq 2\%$ resulted in a higher early-age (3-day) compressive strength but reduced the rate of the hydration reaction, to some extent, compared to mixes with $v_f < 2\%$. It is also worth noting that the strength gains exhibited by the RCA-based mixes having a 3% SF, by volume, were insignificantly different from those exhibited by the NA-based control mix.

The development of the cylinder compressive strength of concrete mixes is illustrated in Fig. 5. It is clear that all mixes, regardless of the percentage of RCA replacement and SF volume fraction, showed a similar strength development profile as that of the control mix R0SF0. Nevertheless, results of Fig. 5 show that the concrete compressive strength at different ages was majorly affected by the RCA content. As expected, the control/reference sample (R0SF0) achieved the highest strength at the age of 3, 7 and 28 days. However, it is worth noting that, although the control

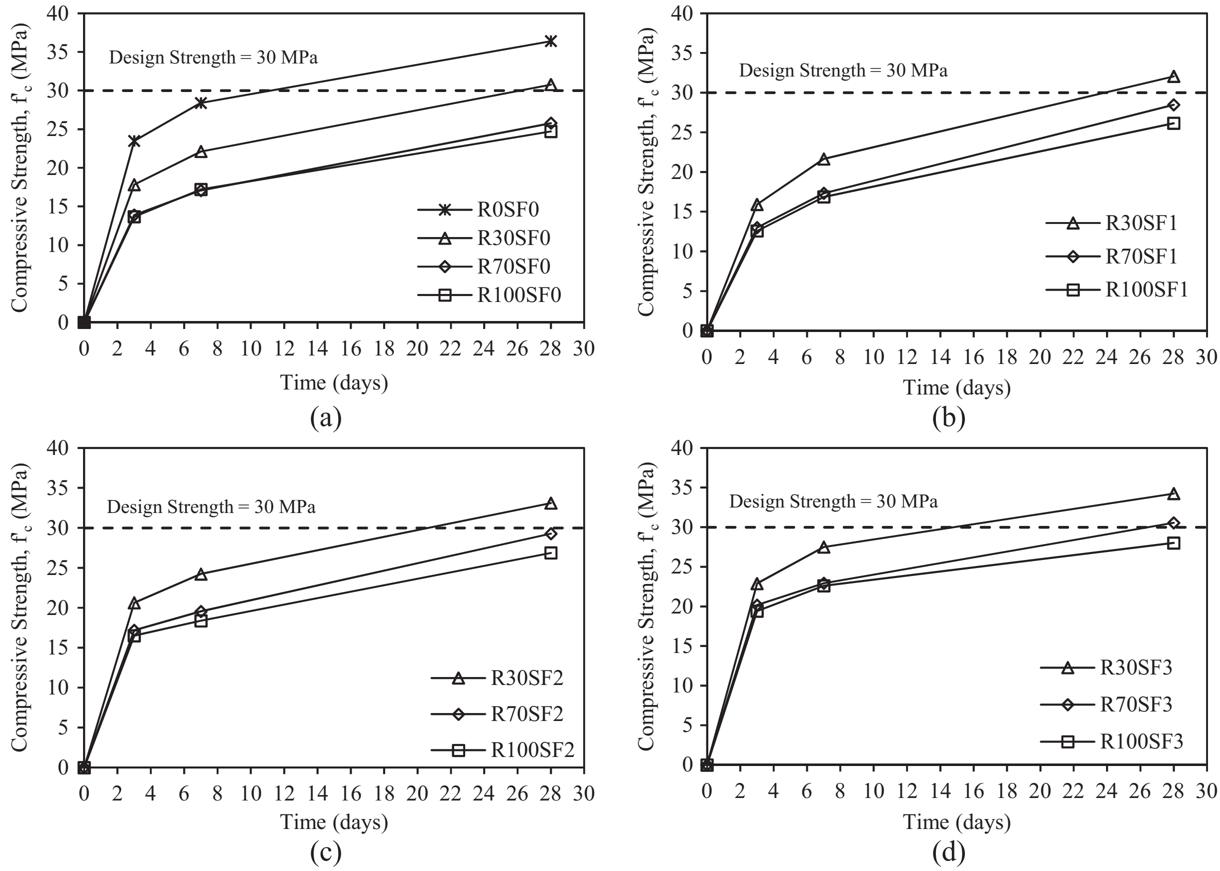

Fig. 5. Development of compressive strength of concrete mixes: (a) SF 0%; (b) SF 1%; (c) SF 2%; (d) SF 3%.

mix was designed to achieve a 28-day design cylinder compressive strength of 30 MPa, as per the procedure of ACI 211.1 [34], the experimental cylinder compressive strength was 21% higher at 36.4 MPa. Apparently, concrete mixtures made with dune sand instead of natural fine aggregates have better particle packing and denser concrete structure [50]. Nevertheless, the experimental strength results are compared to the 28-day design compressive strength (30 MPa), as illustrated in Fig. 5(a). The substitution of 30% of NA with RCA in plain concrete mix R30SF0 did not reduce the strength below the 30 MPa mark. However, mixes with higher RCA replacement percentages failed to achieve the 30-MPa design cylinder strength. This can be attributed to the weak paste-aggregate interface and the rough, porous structure of the RCA.

As shown in Fig. 5(b–d), the addition of SF in volume fractions of 1, 2, and 3% to 30% RCA concrete samples resulted in compressive strengths in the range of 32–34 MPa, thus exceeding the 30-MPa design cylinder strength. Furthermore, concrete mixes with a 70% RCA replacement and SF volume fractions of 1, 2, and 3% were able to achieve 95, 98, and 100% of the 30 MPa design cylinder compressive strength, respectively. Upon complete replacement of NA by RCA (100%), concrete samples with 1, 2, and 3% SF volume fractions achieved 87, 90, and 93% of the 30-MPa design cylinder compressive strength, respectively. The addition of SF provided a denser concrete, evidenced by density and absorption results of Tables 3 and 4. Also, their presence resulted in a better structural integrity due to its bridging effect. Thus, it could be concluded that 100% RCA could be used in steel fiber-reinforced concrete mixes made with desert dune sand and a minimum v_f of 2% while sustaining a maximum loss of 10% in the design cylinder compressive strength. Nevertheless, a lower RCA replacement percentage of 70% could be used in conjunction with a steel fiber volume fraction of 1% to produce concrete with a limited loss of up to 5% in the design cylinder compressive strength. No loss in the design cylinder compressive strength was recorded for mixtures with a 70% RCA replacement and $v_f \geq 2\%$.

The 28-day cube compressive strength, f_{cu}, is also presented in Table 5. Similar to the cylinder compressive strength, increasing the RCA replacement percentage resulted in a reduction in cube strength. The plain concrete mix with 100% RCA (R100SF0) showed a decrease in f_{cu} by 39%. This could be attributed to the old adhered mortar attached to RCA, creating a weak interface zone, and to the poor quality of RCA with abundant cracks and voids. The addition of SF slightly increased f_{cu} of the RCA-based mixtures. On average, the addition of 1, 2 and 3% SF, by volume, resulted in 7, 10 and 14% increases in the cube strengths, respectively, compared to those of their plain RCA-based counterparts. Clearly, RCA replacement had a dominant effect on the concrete compressive strength over the addition of SF. Table 5 also presents the ratio of f'_c/f_{cu}. The NA-based control specimen R0SF0 had a ratio of 0.85. An increase in RCA replacement percentages in plain concrete led to an increase in f'_c/f_{cu}. This indicated that the difference between the cube and cylinder compressive strengths decreased when more RCA was used in the concrete mix. It seems that the confinement effect of cubes in compression is not as apparent when NA is replaced by RCA. Nevertheless, the addition of SF volume fraction of 3% to a concrete mixture having a 30% RCA replacement (R30SF3) could enhance this confinement and produce a concrete with an f'_c/f_{cu} ratio closer to that of the NA-based control counterpart.

The relationship between f'_c and f_{cu} is illustrated in Fig. 6. Clearly, a linear correlation exists between the cylinder and cube compressive strengths. Several models were developed using linear regression analysis for mixes with the same RCA replacement

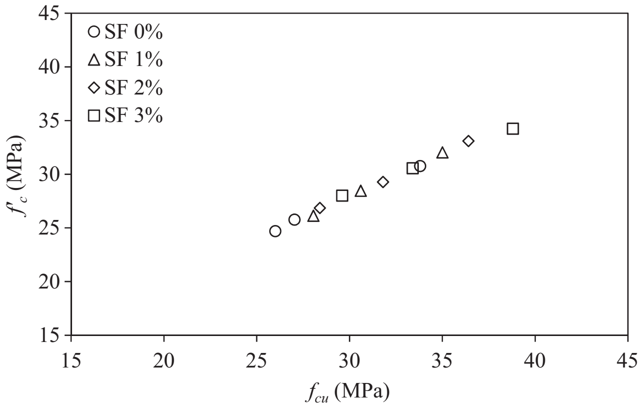

Fig. 6. Relationship between f'_c and f_{cu}.

percentage. Results show that mixes with 30, 70, and 100% RCA have average f'_c/f_{cu} ratios of 0.90, 0.92, and 0.93, respectively. With similar ratios being reported, a single relationship was established to represent all mixes, as shown in Eq. (5). In fact, it could be used to predict the cylinder compressive strength from the cube strength with reasonable accuracy ($R^2 = 0.92$). Nevertheless, a more accurate prediction equation, Eq. (6), was introduced to include a y-intercept with a correlation coefficient, R^2, of 0.99.

$$f'_c = 0.91 f_{cu} \tag{5}$$

$$f'_c = 0.72 f_{cu} + 6.34 \tag{6}$$

In addition to the relationships introduced in Eqs. (5) and (6), prediction equations suggested by Gao et al. [22], Xiao et al. [58] and Xie et al. [59] were employed to estimate the cylinder compressive strength given the cube strength of RCA-based concrete mixtures with and without steel fibers, as shown in Fig. 7. It can be seen that most of previously published equations underestimated the experimental value of f'_c. However, only when f'_c exceeded 32 MPa, the equations by Gao et al. [22] and Xie et al. [59] could be used to provide a reasonable prediction.

3.5. Compressive stress-strain response

Typical axial compressive stress-strain curves of 28-day cylinder concrete specimens are illustrated in Fig. 8. The effect of SF volume fraction on the stress-strain behavior is examined through comparing mixes of 30% RCA replacement [Fig. 8(a)]. In fact, the peak stress increased by an average of approximately 4% for every

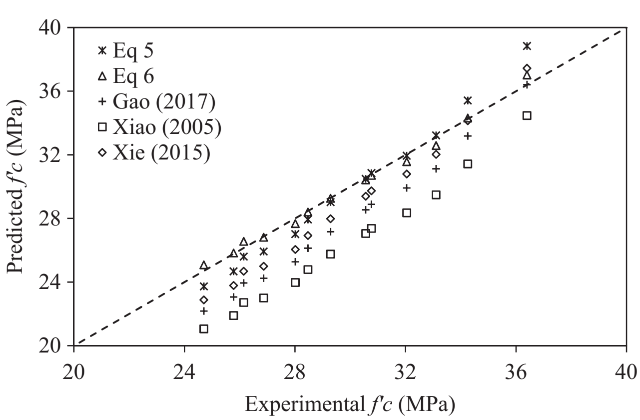

Fig. 7. Predicted versus experimental values of f'_c.

1% SF volume fraction added to concretes with 30% RCA. On the other hand, concrete mixes made with 70% and 100% RCA were associated with increases of approximately 7 and 5% for every 1% SF volume fraction, respectively. While these increases seem insignificant, it should be noted that SF are mainly added to concrete mixes to enhance the deformation capacity due to their bridging effect. Fig. 8(a) also shows the effect of SF addition on the peak stress-strain response. Upon the addition of 1, 2, and 3% SF, the strain at peak increased by 160, 197, and 234%, respectively. On average, each 1% SF added could increase the strain at peak by 98, 46, and 35% for 30, 70, and 100% RCA concrete mixes, respectively. It can be thus concluded that the most significant effect of adding SF was to increase the deformability of RCA concrete mixes, evidenced by the increase in peak strain of mixes with higher volume fractions.

Fig. 8(b) investigates the influence of RCA replacement percentages on the compression behavior of plain concrete samples. In the absence of SF, the peak stress and slope of stress-strain curves decreased as the RCA replacement percentage increased in the mixes. Such reduction can be attributed to the reduction in density and modulus of elasticity of concrete mixes, particularly for the mixes with higher RCA replacement percentage. This is consistent with findings reported in the literature by other researchers [3,8,10,14,58]. Higher RCA replacement yielded a slightly higher peak strain, as low-strength concrete exhibits larger strain at peak load. This also resulted in a reduced elastic modulus. It can be thus concluded that the increase in the SF volume fraction changed the stress-strain response and allowed the specimens to exhibit greater peak strains compared to that of the plain specimens with RCA replacement.

3.6. Modulus of elasticity

The modulus of elasticity, E_c, of concrete mixes with different RCA and SF percentages were obtained from stress-strain curves, using Eq. (7), as per ASTM C469 [43]:

$$E_c\ (\text{MPa}) = \frac{S_2 - S_1}{\varepsilon_2 - 0.00005} \tag{7}$$

where S_2 is the stress corresponding to 40% of the ultimate stress, S_1 is the stress corresponding to a longitudinal strain of 50 millionths and ε_2 is the longitudinal strain produced by the stress S_2.

As shown in Fig. 9, a reduction in the E_c value was noticed with an increase in the percentage of RCA replacement. For plain concrete mixes, 30, 70, and 100% RCA replacements resulted in respective decreases in E_c of 19, 42, and 46% compared to that of the NA-based control mix, R0SF0. This is consistent with other findings reported in previous investigations [58,59]. This reduction in E_c is mainly due to the presence of cement mortar attached to RCA, creating a more porous and less dense concrete structure. Furthermore, the addition of SF by 1, 2 and 3% volume fractions led to average increases of 8, 11 and 17% in E_c, respectively, compared to those of plain RCA-based concrete counterparts. Such increase in the modulus of elasticity of RCA-based specimens containing SF can be attributed to the increase in their compressive strength, which increased the value of S_2, in Eq. (7), and thus their modulus of elasticity. Yet, it should be noted that the increase in the modulus of elasticity of the SF concrete mixes having a 100% RCA replacement percentage was insignificant. Apparently, the effect of RCA replacement on E_c was more prominent than that of SF addition.

Modulus of elasticity results were modeled based on regression analysis. Two models were proposed, as presented in Eqs. (8) and (9), to predict the values of E_c (in GPa) with reasonable accuracy ($R^2 = 0.96$). Eq. (8) relates E_c to f'_c (in MPa) as a linear function with a y-intercept, similar to that proposed by ACI 363 [60]. In compar-

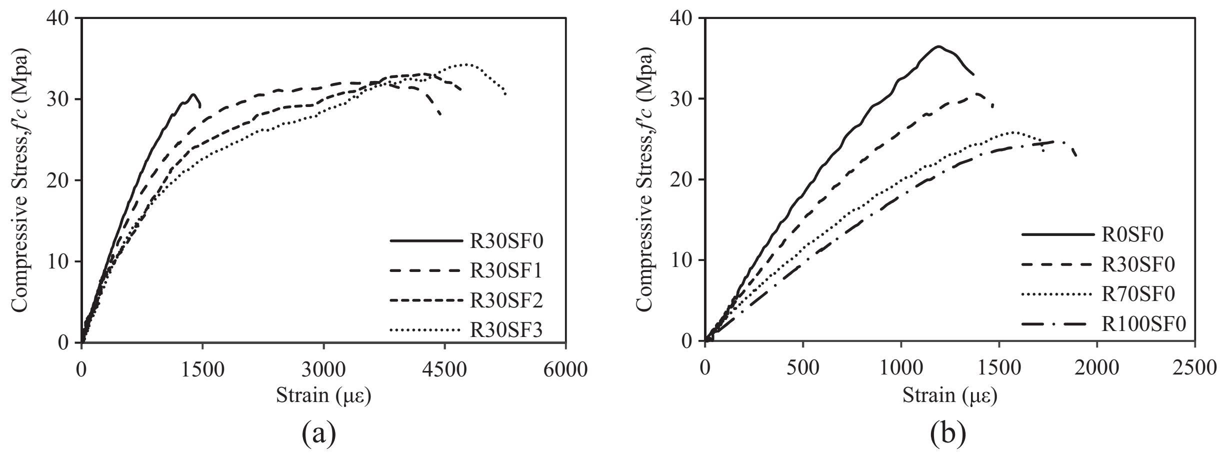

Fig. 8. Typical compression stress-strain curves of cylinder concrete specimens with different (a) SF volume fraction and (b) RCA replacement percentage.

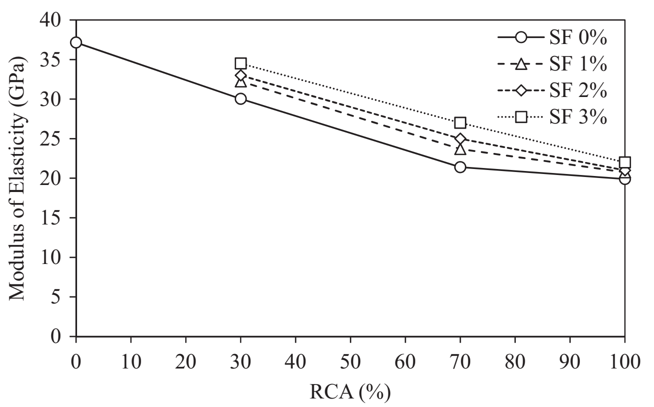

Fig. 9. Modulus of elasticity of concrete mixes with different RCA and SF contents.

ison, Eq. (9) provides similar prediction accuracy but as a power function.

$$E_c = 18.1\sqrt{f'_c} - 71.7 \quad (8)$$

$$E_c = 0.0552 f_c'^{1.8195} \quad (9)$$

The obtained relationships in Eq. (8) and (9) are compared to those developed by ACI Committee 363 [60], ACI Committee 318 [61], Dilli et al. [62], Ahmed and Shah [63], CEB-FIP [64] and Mendis [65]. Fig. 10 presents the predicted versus experimental modulus of elasticity. The equations introduced in this work gave a reasonable accuracy with values converging around the 45°-line. The model suggested by Dilli et al. [62] significantly underestimated the modulus, while those proposed by Ahmed and Shah [63] and Mendis [65] tended to overestimate it. Furthermore, the equation given by the ACI Committee 363 [60] slightly overestimated the modulus for values lower than 22 GPa and accurately predicted the modulus for values between 22 and 30 GPa, after which it underestimated the experimentally obtained modulus of elasticity. Similarly, the model proposed by CEB-FIP [64] overestimated the modulus for experimental values lower than 30 GPa and tended to underestimate modulus of elasticity values higher than 30 MPa. Clearly, the presence of SF and RCA rendered codified and other equations reported in the literature of typical concrete mixes unsuitable.

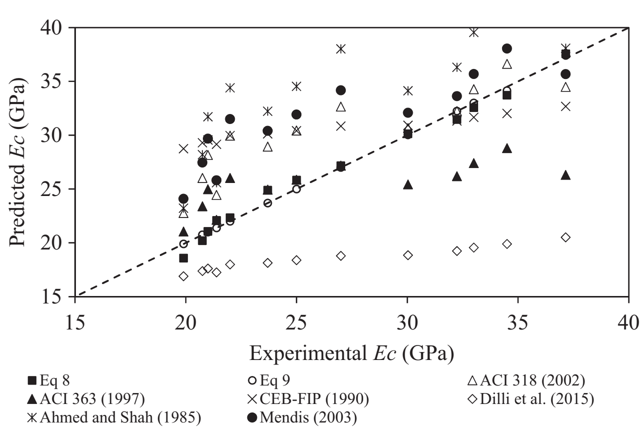

Fig. 10. Correlation between modulus of elasticity and 28-day cylinder compressive strength.

3.7. Ultrasonic pulse velocity and bulk resistivity

The UPV test was used to assess concrete strength and quality. A higher velocity is an indication of a denser concrete mix. It is directly affected by the presence of voids and pores in the concrete matrix and in the aggregates. The results of the UPV test conducted on concrete specimens at the age of 28 days are summarized in Table 6. Results ranged between 2222 and 4831 m/s with lowest and highest velocities recorded for the 100% RCA plain concrete and NA-based control mixes, respectively. For plain RCA-based concrete mixes (v_f = 0%), RCA replacements of 30, 70 and 100% resulted in 34, 51 and 54% respective reductions in the velocity relative to that of the NA-based control specimen. Such a reduction is

Table 6
UPV and bulk resistivity of 28-day concrete samples.

Mix Designation	RA (%)	SF (%)	UPV (m/s)	Bulk Resistivity (kΩ.cm)
R0SF0	0	0	4831	6.3
R30SF0	30	0	3167	4.4
R70SF0	70	0	2353	4.0
R100SF0	100	0	2222	3.8
R30SF1	30	1	3589	-
R70SF1	70	1	2898	-
R100SF1	100	1	2703	-
R30SF2	30	2	4000	-
R70SF2	70	2	3300	-
R100SF2	100	2	2989	-
R30SF3	30	3	4348	-
R70SF3	70	3	3800	-
R100SF3	100	3	3456	-

a direct indication of the increase in void and crack content in samples with higher RCA replacement percentage, which ultimately resulted in lower hardened concrete density, as shown in earlier sections. Nevertheless, Malhotra [66] classified concrete specimens as "good" for UPV values falling in the range of 3660–4580 m/s. Without SF, plain concrete mixes with any RCA replacement fell outside the range. The addition of 2–3% SF volume fraction could, however, produce better quality concrete that falls within the designated range.

The UPV test results were also correlated to the 28-day cylinder compressive strength, so that strength can be estimated through a non-destructive test method. As shown in Fig. 11, a strong linear correlation exists between these two properties with a correlation coefficient, R^2, value as high as 0.91. Eq. (10) presents the proposed linear regression equation to predict f'_c (MPa) using the velocity, v (m/s), values. With a continuously increasing linear equation, it is clear that a denser concrete mix, characterized by a higher UPV value, leads to a higher compressive strength. Nevertheless, such equation could be of great value to the construction industry to anticipate the performance of sustainable concrete made with RCA, dune sand, and SF without the need for extensive experimental testing.

$$f'_c = 0.0044v + 14.854 \tag{10}$$

Results of bulk resistivity experimental testing are also shown in Table 6. As noted earlier, SF are electrically conductive materials and may produce unrepresentative results. Therefore, only plain mixes with and without RCA were considered in this experiment. Values ranged between 3.8 and 6.3 kΩ.cm. Apparently, the bulk resistivity of concrete was affected by the presence of RCA. In fact, 30, 70, and 100% RCA replacement led to 30, 36, and 40% reductions in the bulk resistivity, respectively, compared with that of the NA-based concrete specimen. This is mainly due to the rough, porous surface texture of RCA, in addition to the weak interface zone between the old and new cement paste, which resulted in large amount of pores present in RCA concrete mixes, higher water absorption, and reduced mechanical properties. Although the lowest RCA substitution (30%) had a significant impact on resistivity, higher percentages of 70 and 100% did not seem to affect it proportionally. It is possible that the increase in pore space when a 30% RCA replacement percentage was used had severely lowered the resistivity to the extent that higher replacement percentages could not cause further severe reduction.

3.8. Abrasion resistance

Fig. 12 shows the abrasion resistance of various concrete mixes incorporating different quantities of RCA and SF. Results showed that higher RCA content led to more abrasion mass loss. Compared to R0SF0 mix, plain concrete specimens with 30, 70, and 100% RCA replacement exhibited 2, 8, and 36% increases in mass loss due to abrasion, respectively. This is mainly associated to the weaker abrasion resistance of the RCA compared to the NA, as noted in Table 1, and the inferior hardened properties of the RCA-based concrete specimens compared to those of the NA-based control specimen. As shown in Fig. 12, the addition of SF considerably improved the abrasion resistance of RCA concrete mixes, as manifested by the significant reduction in their abrasion mass loss relative to those of their plain RCA-based counterparts. For concrete mixes with a 30% RCA replacement percentage, increasing the SF volume fraction from 1 to 3% did not result in a further increase in the abrasion resistance (i.e. the abrasion mass loss of these specimens were insignificantly different). An average reduction of 47% in the abrasion mass loss was recorded for these specimens compared to that of the plain RCA-based counterparts, irrespective of SF content. Yet, the effect of adding SF was different in concretes with higher RCA replacement. The addition of 1%, 2% and 3% of SF, by volume, in concrete mixes having a 100% RCA replacement percentage resulted in respective reductions of 27, 40 and 47% in abrasion mass loss compared to that of the plain RCA-based counterparts. It seems that adding SF maintained better geometric integrity of concrete samples, owing to the bridging effect of SF. As a result, steel fiber-reinforced RCA concrete specimens were more resistant to abrasion.

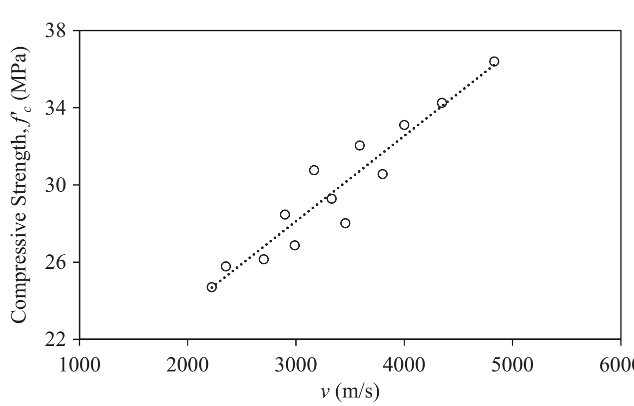

Fig. 11. Relationship between UPV and f'_c.

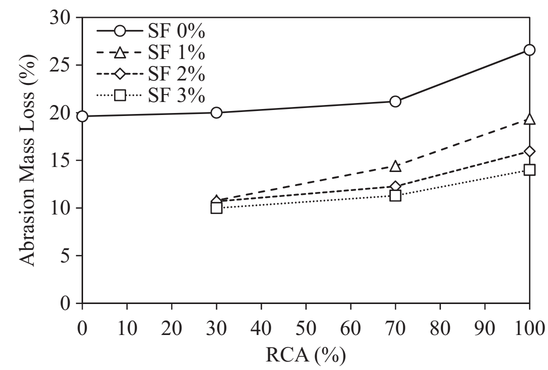

Fig. 12. Effect of RCA and SF percentages on the abrasion resistance of concrete.

4. Conclusions

Different fresh and hardened properties of plain and steel fiber-reinforced concrete made of RCA and dune sand were examined in this paper. Based on tests results, the following conclusions can be drawn:

- Fresh and hardened concrete densities and slump decreased as more NA was replaced with RCA. The addition of SF resulted in an increase in fresh and hardened concrete densities but further reduced the slump. A regression model capable of predicting the hardened 28-day concrete density from the fresh density was introduced.
- Water absorption and the initial sorptivity were increased by approximately 8% for every 10% RCA replacement percentage. The addition of SF improved the hardened properties of RCA concrete by reducing the water absorption and the initial sorptivity by an average of approximately 7.5 and 9%, respectively, for every 1% SF added.
- The incorporation of SF resulted in higher early age cylinder compressive strength but limited the development of hydration reaction. RCA replacement had a dominant impact on the com-

pressive strength over SF addition, with a reduction in strength due to the former outweighing the strength gain due to the latter.

- The replacement of 30% of NA with RCA in plain concrete did not result in a reduction in the design cylinder compressive strength of 30 MPa. Mixes with higher RCA replacement percentages failed to achieve the 30-MPa design cylinder strength.
- A RCA replacement percentage of 70% could be used in conjunction with a steel fiber volume fraction of 1% to produce concrete with a limited loss of up to 5% in the design cylinder compressive strength. No loss in the design cylinder compressive strength was recorded for mixtures with a 70% RCA replacement and $\upsilon_f \geq 2\%$.
- For concrete mixes with a 100% RCA replacement percentage, a minimum steel fiber volume fraction of 2% is needed to sustain a maximum loss of 10% in the design cylinder compressive strength.
- An increase in RCA replacement percentage in plain concrete mixes resulted in an increase in f'_c/f_{cu} ratio, signifying a reduction in confinement effect. The addition of υ_f of 3% could enhance the confinement effect and produce a concrete with a f'_c/f_{cu} ratio closer to that of the NA-based counterpart. Two regression models were introduced to predict the cylinder compressive strength from the cube compressive strength with a reasonable to high accuracy (R^2 = 0.92 and 0.99). These models provided a more realistic approach compared to other models available in the literature.
- The experimental compressive stress-strain curves showed that the increase in RCA replacement percentage in plain concrete mixes resulted in a lower peak stress but slightly higher strains at peak. The addition of SF significantly increased the strain at peak stress.
- The elastic modulus decreased with higher RCA replacement percentages. For 30, 70, and 100% RCA replacement, it was reduced by 19, 42, and 46%, respectively. The addition of SF slightly increased the elastic modulus, with an average of 6% increase for every 1% SF added. Accordingly, the effect of RCA replacement on elastic modulus was more prominent than that of SF addition. Two models were introduced by linear and power regression analyses to estimate the 28-day elastic modulus of steel fiber-reinforced recycled aggregate concrete mixes.
- UPV and bulk resistivity values decreased with an increase in the RCA replacement percentages, possibly due to an increase in voids and cracks content. The quality of the concrete, through UPV, could be notably improved by adding SF. Regression models were introduced to correlate UPV value with the 28-day cylinder compressive strength.
- Mass loss due to abrasion increased with the RCA replacement percentages. This inferior abrasion resistance of plain RCA-based concrete was improved through the addition of SF, owing to better geometric integrity and bridging effect of SF.

Based on the research findings, concrete made with 100% RCA, steel fiber reinforcement, and desert dune sand could be developed with fresh and hardened properties comparable to those of the conventional concrete. Future studies will focus on the flexural and tensile performance of steel fiber-reinforced RCA concrete mixes. Lifecycle assessment and cost-benefit analysis are also critical aspects to the potential applications of such concrete and warrant separate studies in the future.

Conflict of interest

The authors wish to confirm that there are no known conflicts of interest associated with this publication.

Acknowledgements

This project is supported by the United Arab Emirates University (UAEU) [grant number 31N258]. The authors are thankful to Al Dhafra Recycling Facilities for providing the recycled concrete aggregates. The contributions of the UAEU engineers and staff are also greatly appreciated.

References

[1] V. Radonjanin, M. Malešev, S. Marinković, A.E.S. Al Malty, Green recycled aggregate concrete, Constr. Build. Mater. 47 (2013) 1503–1511.
[2] C. Meyer, The greening of the concrete industry, Cem. Concr. Compos. 31 (8) (2009) 601–605.
[3] M. Casuccio, M.C. Torrijos, G. Giaccio, R. Zerbino, Failure mechanism of recycled aggregate concrete, Constr. Build. Mater. 22 (7) (2008) 1500–1506.
[4] M.S. de Juan, P.A. Gutiérrez, Study on the influence of attached mortar content on the properties of recycled concrete aggregate, Constr. Build. Mater. 23 (2) (2009) 872–877.
[5] F. Debieb, L. Courard, S. Kenai, R. Degeimbre, Mechanical and durability properties of concrete using contaminated recycled aggregates, Cem. Concr. Compos. 32 (6) (2010) 421–426.
[6] A.M. Wagih, H.Z. El-Karmoty, M. Ebid, S.H. Okba, Recycled construction and demolition concrete waste as aggregate for structural concrete, HBRC J. 9 (3) (2013) 193–200.
[7] A. Rao, K.N. Jha, S. Misra, Use of aggregates from recycled construction and demolition waste in concrete, Resour. Conserv. Recycl. 50 (1) (2007) 71–81.
[8] M. Etxeberria, E. Vázquez, A. Marí, M. Barra, Influence of amount of recycled coarse aggregates and production process on properties of recycled aggregate concrete, Cem. Concr. Res. 37 (5) (2007) 735–742.
[9] Ö. Çakır, Experimental analysis of properties of recycled coarse aggregate (RCA) concrete with mineral additives, Constr. Build. Mater. 68 (2014) 17–25.
[10] V. Corinaldesi, Mechanical and elastic behaviour of concretes made of recycled-concrete coarse aggregates, Constr. Build. Mater. 24 (9) (2010) 1616–1620.
[11] M. Malešev, V. Radonjanin, S. Marinković, Recycled concrete as aggregate for structural concrete production, Sustainability 2 (5) (2010) 1204.
[12] S.W. Tabsh, A.S. Abdelfatah, Influence of recycled concrete aggregates on strength properties of concrete, Constr. Build. Mater. 23 (2) (2009) 1163–1167.
[13] F. Bencardino, L. Rizzuti, G. Spadea, R.N. Swamy, Stress-strain behavior of steel fiber-reinforced concrete in compression, J. Mater. Civ. Eng. 20 (3) (2008) 255–263.
[14] G.-F. Belén, M.-A. Fernando, C.L. Diego, S.-P. Sindy, Stress–strain relationship in axial compression for concrete using recycled saturated coarse aggregate, Constr. Build. Mater. 25 (5) (2011) 2335–2342.
[15] B. González-Fonteboa, F. Martínez-Abella, Concretes with aggregates from demolition waste and silica fume. Materials and mechanical properties, Build. Environ. 43 (4) (2008) 429–437.
[16] C.V. Umadevi, M.R. Gowda, Study on strength characteristics of recycled aggregate concrete using polypropylene fiber, Civ. Eng. Technol. Res. 2 (1) (2014) 259–266.
[17] C. Shi, Y. Li, J. Zhang, W. Li, L. Chong, Z. Xie, Performance enhancement of recycled concrete aggregate – a review, J. Clean. Prod. 112 (2016) 466–472.
[18] V.W.Y. Tam, C.M. Tam, Y. Wang, Optimization on proportion for recycled aggregate in concrete using two-stage mixing approach, Constr. Build. Mater. 21 (10) (2007) 1928–1939.
[19] d.P. Marco, C. Matteo, D. Daniele, Fibre-reinforced concrete in fib Model Code 2010: principles, models and test validation, Struct. Concr. 14 (4) (2013) 342–361.
[20] M.S. Meddah, M. Bencheikh, Properties of concrete reinforced with different kinds of industrial waste fibre materials, Constr. Build. Mater. 23 (10) (2009) 3196–3205.
[21] D. Gao, L. Zhang, M. Nokken, Mechanical behavior of recycled coarse aggregate concrete reinforced with steel fibers under direct shear, Cem. Concr. Compos. 79 (2017) 1–8.
[22] D. Gao, L. Zhang, M. Nokken, Compressive behavior of steel fiber reinforced recycled coarse aggregate concrete designed with equivalent cubic compressive strength, Constr. Build. Mater. 141 (2017) 235–244.
[23] M. Ahmadi, S. Farzin, A. Hassani, M. Motamedi, Mechanical properties of the concrete containing recycled fibers and aggregates, Constr. Build. Mater. 144 (2017) 392–398.
[24] J.A. Carneiro, P.R.L. Lima, M.B. Leite, R.D. Toledo Filho, Compressive stress–strain behavior of steel fiber reinforced-recycled aggregate concrete, Cem. Concr. Compos. 46 (2014) 65–72.
[25] P.K. Mehta, J.P. Monteiro, Concrete Microstructure, Properties and Material, McGraw Hill, New York, 2006.
[26] ACI Committee 201.2, Guide to Durable Concrete, American Concrete Institute, Farmington Hills, MI, 2016, p. 87.
[27] ASTM, Standard Specification for Concrete Aggregates C33, ASTM International, West Conshohocken, PA, 2016.
[28] ASTM, Standard Test Method for Soundness of Aggregates by Use of Sodium Sulfate or Magnesium Sulfate C88, ASTM International, West Conshohocken, PA, 2013.

[29] ACI Committee E-701, Aggregates for Concrete, American Concrete Institute, Farmington Hills, Michigan, 2016, p. 30.
[30] M.S. Hossain, D.S. Lane, B.N. Schmidt, Use of the micro-deval test for assessing the durability of virginia aggregates, in: V.T.R. Council (Ed.), Virginia Transportation Research Council Charlottesville Virginia, 2007, p. 33.
[31] ASTM, Standard Test Method for Resistance to Degradation of Small-Size Coarse Aggregate by Abrasion and Impact in the Los Angeles Machine C131, ASTM International, West Conshohocken, PA, 2014.
[32] ASTM, Standard Test Method for Relative Density (Specific Gravity) and Absorption of Coarse Aggregate C127, ASTM International, West Conshohocken, PA, 2015.
[33] Bekaert, Dramix 3D 65/35 Report, Bekaert, Belgium, 2012, p. 1.
[34] ACI Committee 211.1, Standard Practice for Selecting Proportions for Normal, Heavyweight, and Mass Concrete, American Concrete Institute, Farmington Hills, Michigan, 2009.
[35] ASTM, Standard Practice for Making and Curing Concrete Test Specimens in the Laboratory C192, ASTM, West Conshohocken, PA, 2015.
[36] ASTM, Standard Test Method for Slump of Hydraulic-Cement Concrete C143, ASTM International, West Conshohocken, PA, 2015.
[37] ACI Committee 544, Report on the Measurement of Fresh State Properties and Fiber Dispersion of Fiber-Reinforced Concrete, American Concrete Institute, Farmington Hills, MI, 2017, p. 25.
[38] ASTM, Standard Test Method for Density (Unit Weight), Yield, and Air Content (Gravimetric) of Concrete C138, ASTM International, West Conshohocken, PA, 2017.
[39] ASTM, Standard Test Method for Density, Absorption, and Voids in Hardened Concrete C642, ASTM International, West Conshohocken, PA, 2013.
[40] ASTM, Standard Test Method for Measurement of Rate of Absorption of Water by Hydraulic-Cement Concretes C1585, ASTM International, West Conshohocken, PA, 2013.
[41] British Standard, Testing Hardened Concrete – Compressive Strength of Test Specimens, BS EN 12390–3, British Standard, London, UK, 2009.
[42] ASTM, Standard Test Method for Compressive Strength of Cylindrical Concrete Specimens C39, ASTM, West Conshohocken, PA, 2015.
[43] ASTM, Standard Test Method for Static Modulus of Elasticity and Poisson's Ratio of Concrete in Compression C469, ASTM, West Conshohocken, PA, 2014.
[44] ASTM, Standard Test Method for Pulse Velocity Through Concrete C597, ASTM, West Conshohocken, PA, 2016.
[45] ASTM, Standard Test Method for Bulk Electrical Conductivity of Hardened Concrete C1760, ASTM International, West Conshohocken, PA, 2012.
[46] M. Safiuddin, B. Scott, Abrasion resistance of concrete – design, construction, and case study, Concr. Res. Lett. 6 (3) (2015) 136–148.
[47] C. Yalcinkaya, J. Sznajder, A. Beglarigale, O. Sancakoglu, H. Yazici, Abrasion Resistance of reactive powder concrete: the influence of water-to-cement ratio and steel micro-fibers, Adv. Mater. Lett. 5 (6) (2014) 345–351.
[48] ASTM, Standard Test Method for Determining Potential Resistance to Degradation of Pervious Concrete by Impact and Abrasion C1747, ASTM International, West Conshohocken, PA, 2013.
[49] ACI 211.1, Standard Practice for Selecting Proportions for Normal, Heavyweight, and Mass Concrete, American Concrete Institute, Farmington Hills, Michigan, 2002.
[50] F.J. Luo, L. He, Z. Pan, W.H. Duan, X.L. Zhao, F. Collins, Effect of very fine particles on workability and strength of concrete made with dune sand, Constr. Build. Mater. 47 (2013) 131–137.
[51] S. Ismail, M. Ramli, Engineering properties of treated recycled concrete aggregate (RCA) for structural applications, Constr. Build. Mater. 44 (2013) 464–476.
[52] S. Manzi, C. Mazzotti, M.C. Bignozzi, Short and long-term behavior of structural concrete with recycled concrete aggregate, Cem. Concr. Compos. 37 (2013) 312–318.
[53] İ. Şanal, Performance of macrosynthetic and steel fiber-reinforced concretes emphasizing mineral admixture addition, J. Mater. Civ. Eng. 30 (6) (2018) 04018101.
[54] P. Ramadoss, K. Nagamani, Tensile strength and durability characteristics of high-performance fiber reinforced concrete, Arab. J. Sci. Eng. 41 (17) (2008) 307–319.
[55] A. Katz, Properties of concrete made with recycled aggregate from partially hydrated old concrete, Cem. Concr. Res. 33 (5) (2003) 703–711.
[56] N.S. Martys, C.F. Ferraris, Capillary transport in mortars and concrete, Cem. Concr. Res. 27 (5) (1997) 747–760.
[57] N. Tamrakar, The Effect of Steel Fibers Type and Content on the Development of Fresh and Hardened Properties and Durability of Self-consolidating Concrete, Civil Engineering, Ryerson University, Toronto, ON, 2012, p. 144.
[58] J. Xiao, J. Li, C. Zhang, Mechanical properties of recycled aggregate concrete under uniaxial loading, Cem. Concr. Res. 35 (6) (2005) 1187–1194.
[59] J.-H. Xie, Y.-C. Guo, L.-S. Liu, Z.-H. Xie, Compressive and flexural behaviours of a new steel-fibre-reinforced recycled aggregate concrete with crumb rubber, Constr. Build. Mater. 79 (2015) 263–272.
[60] ACI Committee 363, State of the Art Report on High-Strength Concrete, Farmington Hills, MI, 1992, pp. 364-411
[61] ACI Committee 318, Building Code Requirements for Structural Concrete and Commentary, American Concrete Institute, Farmington Hills, Michigan, 2014.
[62] M.E. Dilli, H.N. Atahan, C. Şengül, A comparison of strength and elastic properties between conventional and lightweight structural concretes designed with expanded clay aggregates, Constr. Build. Mater. 101 (2015) 260–267.
[63] S.H. Ahmed, S.P. Shah, Structural properties of high strength concrete and its implications for precast prestressed concrete, PCI J. 30 (6) (1985) 97–123.
[64] CEB-FIP, Evaluation of the Time Dependent Behavior of Concrete, Fib, Lausanne, Switzerland, 1990.
[65] P. Mendis, Design of high-strength concrete members: state-of-the-art, Prog. Struct. Mat. Eng. 5 (1) (2003) 1–15.
[66] V.M. Malhotra, Testing Hardened Concrete: Nondestructive Methods, Iowa State University Press, Iowa, USA, 1976.